

1.B Bounce-Coated Ablation Layers on Fusion Targets

An ablation layer coated on a laser-fusion target must be sufficiently uniform to avoid creating hydrodynamic instabilities during implosion.¹ Any coating method employed should preserve the high degree of sphericity and uniformity obtainable in the starting shell.^{2,3} The principal means used to achieve uniform ablation layers on spherical shells has been to bounce the shells on a vibrating surface while they are being coated, so that all sides are identically exposed to the coating process.⁴⁻¹⁰ Keeping these very light ($\sim 10^{-6}$ g) shells from sticking to the surface or to each other during the coating process requires a variety of strategies, including vertical acceleration of the surface sufficient to overcome sticking forces,⁴ a plasma to prevent a large surface charge from arising, and others to be discussed.

The low-Z polymer parylene¹¹ is often used for ablation layers, but is not conventionally applied in the presence of a plasma. Maintaining a low-power plasma sufficient to overcome sticking due to surface charge modifies the parylene coating process considerably, as evidenced by a large increase in coating rate and embrittlement of the coating. This report describes the role of the plasma in the coating process and some of the properties of the coating that result from the use of the plasma.

Description of Bounce Coating

The physical arrangement of the bounce-coating apparatus is shown in Ref. 5. Parylene monomer enters the coating chamber, prepared as in the conventional parylene process. Argon is also bled in to maintain a pressure of 36 mTorr. A plasma is generated by applying a low-frequency sinusoidal voltage between a flat electrode 5 cm above the shells and the surface on which the shells bounce. Turning on the plasma reduces the monomer pressure (observable on a heated gauge) while increasing the coating rate. The parylene monomer absolute pressure is unknown, but is calculated to be ~ 12 mTorr with the plasma off. This value is determined from the measured coating rate and the known relationship among coating rate, substrate temperature, and monomer pressure.¹¹ The plasma is maintained at a low power (~ 200 mW) because a higher power causes particles to form in the vapor. A lower power, on the other hand, is difficult to maintain and results in an increased probability for the lightest shells to stick. To keep out contaminants, shells are inserted and extracted without exposing the coating region to air.

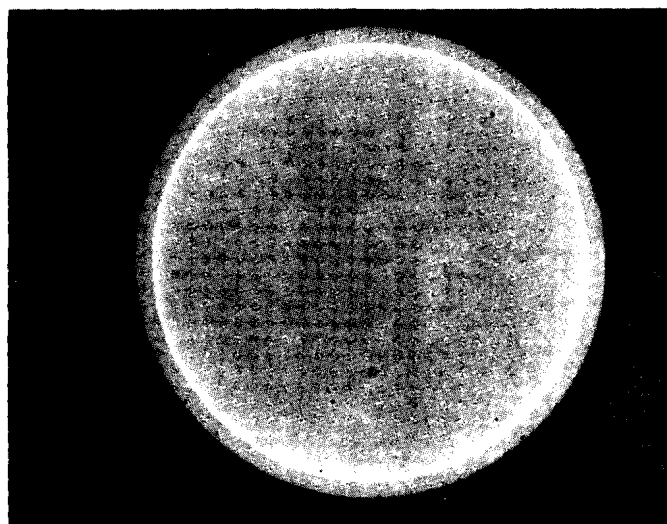
The shells (up to 20 at a time) bounce on the vertically vibrating surface of a mechanical resonator.^{4,5} The principal advantage of this resonator over other types of vibrating surfaces is that vertical motion is relatively uniform over the entire surface of area 20 cm^2 . This uniformity is assured by the nature of the longitudinal mode of vibration used. A constant vibrational amplitude is maintained by a feedback loop. Too high a peak surface velocity can throw shells out of the coating region. To protect against target losses, a thin-foil catcher is glued around the upper edge of the mechanical resonator, increasing its radius by 70%. The foil surface does not vibrate enough

to bounce shells, but a shell accidentally thrown there can be picked up with the probe and returned to the bouncing region. Use of the foil allows use of a peak acceleration of $5 \times 10^3 \text{ m/s}^2$ at 20 kHz, which is usually sufficient to keep the lightest shells ($0.3 \times 10^{-6} \text{ g}$) bouncing.

A microscope is set up for observing the bouncing shells, allowing the operator to intervene if sticking occurs. Solid glass spheres ($\sim 240\text{-}\mu\text{m}$ diameter) bounced along with the shells help prevent sticking. If these strategies fail and targets stick, a thin-fiber probe can be manipulated from outside the coating chamber and used to unstick shells without stopping the coating. This method of unsticking is avoided if possible, however, since shells unstuck in this manner after parylene has bonded them to the surface may be left with flaws. Surface flaws can grow as bounce coating proceeds, a process well characterized by others.⁷ The preferred way to overcome sticking is to maintain a sufficient vertical acceleration.

The coating thickness is monitored during coating by a reflectometer.¹² The shells, well characterized prior to being coated, are reidentified to the extent possible by diameter measurement and x-ray radiography.¹³ A typical radiograph, shown in Fig. 34.12, indicates the high degree of uniformity attained. The best coatings are free of surface features larger than $\sim 0.2 \mu\text{m}$ in height. The appearance of the surface is slightly smoother than is seen in Ref. 5.

Fig. 34.12
X-ray radiograph of a bounce-coated
glass shell.



← 100 μm →

T796

Role of the Plasma

Maintaining a suitable plasma power during a coating run that lasts several hours requires either automatic control or frequent operator attention. Figure 34.13 shows how the plasma current is measured and controlled. The small plasma current used here ($\sim 0.3 \text{ mA rms}$) is an order of magnitude smaller than the current drawn by capacitive elements of the circuit. In the circuit shown here, the phase of the lock-in amplifier is adjusted so that the output is zero if the plasma is

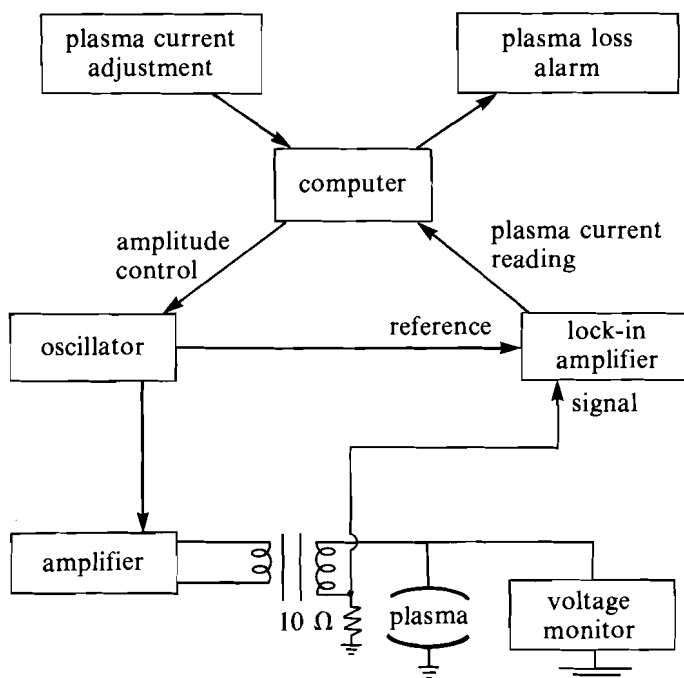
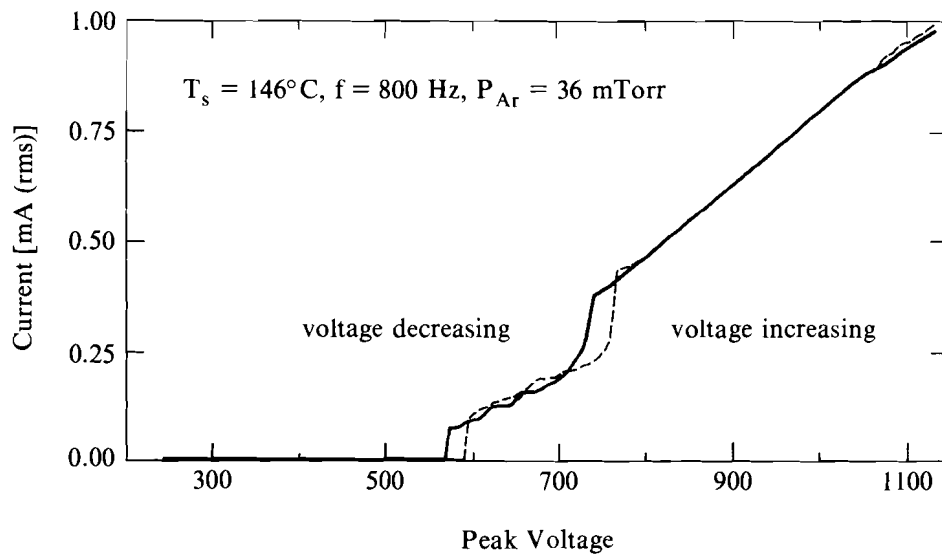


Fig. 34.13
Circuit for measuring the plasma and closed-loop feedback for maintaining the plasma.

T804

off. This can be done because at low plasma currents, the two currents differ in phase by 90° . (The phase difference is verified by observing that the lock-in amplifier, when its phase is switched by 90° , is insensitive to the plasma being on or off.) The rms plasma current is then the rms voltage read by the lock-in divided by the resistance to ground of $10\ \Omega$. At low plasma currents, the current flows only at peak drive voltage, so the plasma power is given by the product of rms plasma current and peak voltage. At the frequency used here, 800 Hz, a low-power plasma is intermittent, consisting of two short current spikes per cycle. When the drive voltage is increased above the values used here, the waveform of the current becomes more complicated and the reading on the lock-in is no longer an accurate measure of plasma current.

The current-voltage characteristic for typical operating conditions of the coating process is shown in Fig. 34.14. The current is an rms value at the drive frequency of 800 Hz. The dimer sublimation temperature T_s controls the rate at which monomer enters the coating region. The argon pressure P_{Ar} is measured on a gauge separated from the coating region by a small cold trap that prevents monomer from reaching the gauge. The characteristic curve exhibits two bistable regions, the lower of which is a threshold for the plasma to turn on or off. An operating point just below or within the upper bistable region is commonly used. The bistability causes some difficulty in controlling the plasma, and it is sometimes necessary to tolerate fluctuating values of current as a result. Operating near the lower bistable region risks



T863

Fig. 34.14
Current-voltage characteristic of parylene-argon plasma showing two bistable regions. The data were taken using a slow sweep of the drive voltage. The bistable regions are not a result of any time constant of the instrumentation.

plasma loss and consequent target sticking. Families of curves like Fig. 34.14 have been taken using various values of T_s and P_{Ar} . There are values of these parameters for which the lower bistable region spans a much wider voltage range, for instance at low values of P_{Ar} . Avoiding this wider bistable region is one of the considerations leading to the choice of operating parameters.

The coating rate varies strongly with both plasma power and monomer pressure. It is seen in Fig. 34.15 that starting the plasma more than doubles the coating rate. The coating rate increases rapidly with increasing power, but then begins to level off, suggesting a partial depletion of the supply of incoming monomer. At high coating rates and plasma power, particles of unknown composition form in the coating region. Each curve in Fig. 34.15 has a threshold for particle formation, which is detected visually. Raising the power much above this threshold causes extremely rapid particle formation. Avoiding particle formation is facilitated by finding a chamber and electrode geometry in which the likeliest spot for particle deposition is readily observed and is far away from the targets. The point on Fig. 34.15 usually used for bounce coating is a power of 200 mW and a coating rate of $2\ \mu\text{m/h}$, conditions under which no particle formation occurs.

Bounce-Coated Polymer Shells

Polymer shells bounce coated with parylene are given added strength by the parylene and so can be permeated with gas to a higher internal pressure. For some gases, parylene can also function as a barrier layer that increases the permeation-time constant by a useful amount. It cannot be assumed that the properties of importance here, permeability and tensile strength, are the same for plasma-deposited parylene as for conventional parylene.

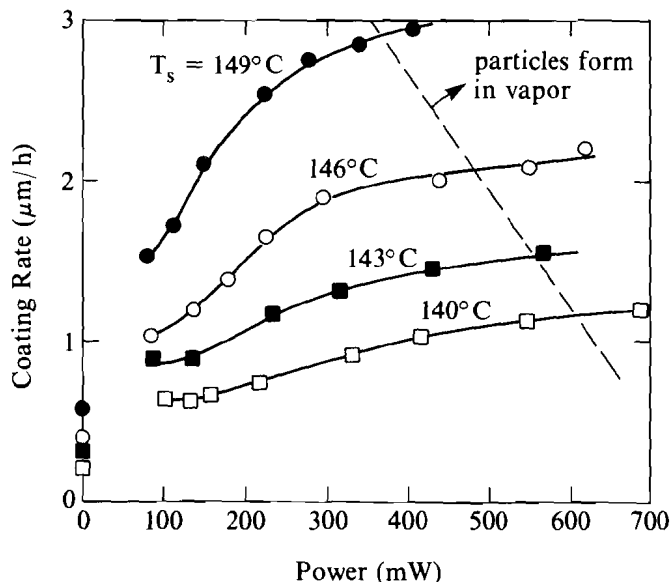


Fig. 34.15

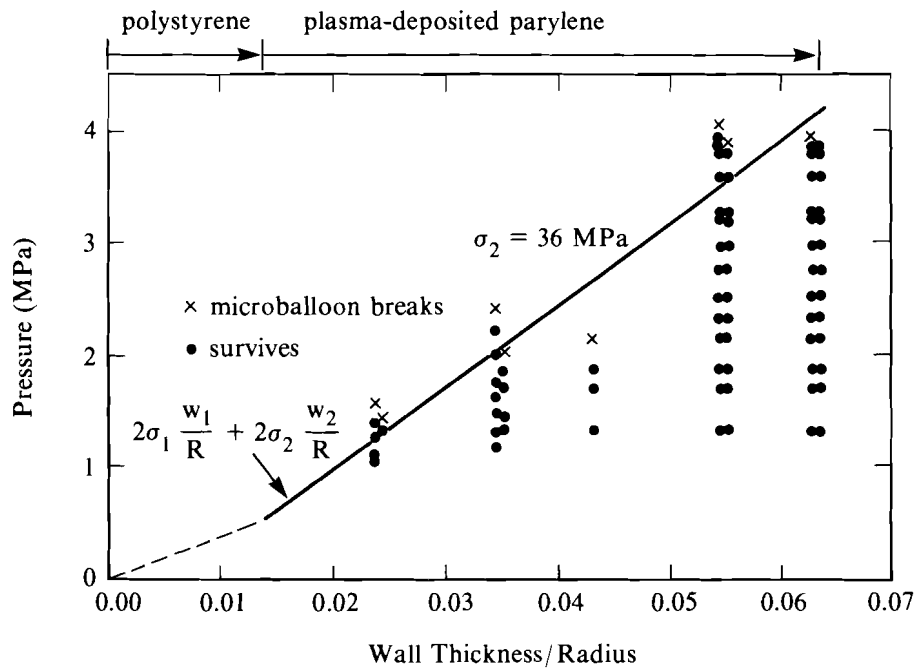
Variation of coating rate with plasma power and sublimation temperature at $P_{Ar} = 36$ mTorr. The points at zero plasma power represent the conventional parylene process.

T861

To measure tensile strength, a set of polystyrene shells made at Lawrence Livermore National Laboratory² was selected in a narrow range of diameters (472 to 496 μm) and wall thicknesses (3.3 to 3.5 μm, measured with single-direction interferometry). These were bounce coated with five different thicknesses of parylene in the range 2.4 to 12.0 μm. The shells were then permeated with He to various pressures, individually or in small groups, and kept under pressure a long enough time so that the internal pressure would be within 1% of the external pressure. The external pressure was released in 1 to 2 s, a time short enough that no significant internal pressure was lost. Survival or failure of each shell was noted, and the pressure plotted in Fig. 34.16. If the assumption is made that the strengths of polystyrene and parylene may be simply added, the points of highest pressure survival are fitted by

$$P_{\max} = 2 \sigma_1 \frac{w_1}{R} + 2 \sigma_2 \frac{w_2}{R}, \quad (1)$$

where the subscript 1 refers to polystyrene and subscript 2 to parylene, σ = tensile strength, w = wall thickness, and R = radius. The radii of the two materials are close enough to be treated as equal. Equation (1) may be understood by equating the force trying to push apart two halves of a thin-walled spherical shell, $\pi R^2 P$, with the strength of the wall where the hemispheres join, $2\pi R(w_1 \sigma_1 + w_2 \sigma_2)$. A least-squares fit of Eq. (1) to the data in Fig. 34.16 yields tensile strengths $\sigma_2 = 36$ MPa for plasma-deposited parylene and an extrapolated value of $\sigma_1 = 18$ MPa for polystyrene. The value for plasma-deposited parylene is 80% of the value listed for conventional parylene. The strength for any given shell may be limited by the intrinsic strength of



T864

Fig. 34.16

Survival of polymer shells with internal pressure. The shells are polystyrene bounce coated with various thicknesses of parylene. A fit of the highest-pressure survival data (solid line for the parylene portion, dashed line for polystyrene) to Eq. (1) yields values of the tensile strengths of the materials. The pressure shown is internal minus external pressure.

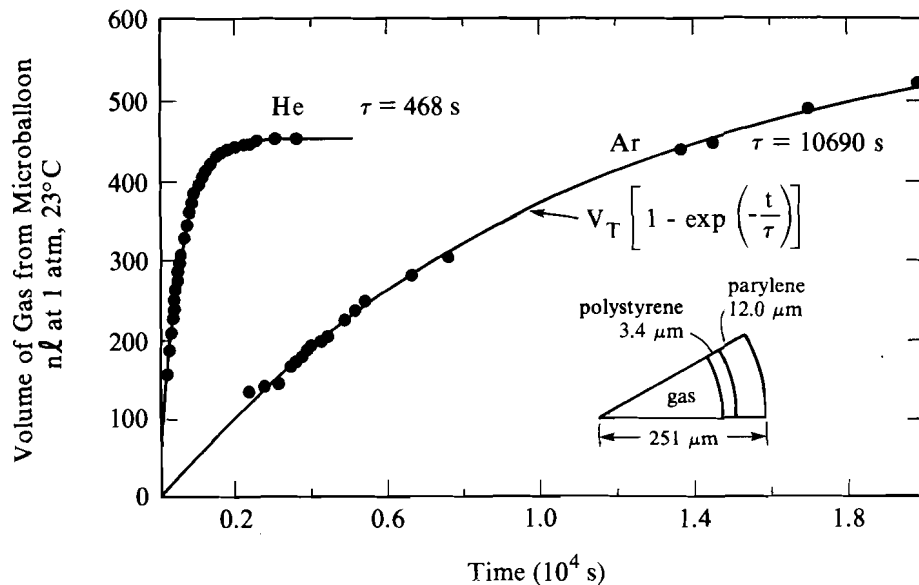
the materials or by a flaw from which a fracture can spread. This may partially account for the scatter in the data.

The tensile strength measurements required knowledge of lower and upper limits for the permeability of plasma-deposited parylene to He gas. To obtain values of permeability, several shells that had already survived permeation to moderate or high pressures were permeated again with He or Ar, and their outpermeation was measured as a function of time. The measurement was based on a method described by E. Lilley,^{2,14} in which a shell is placed in the closed end of a glass capillary tube and permeated with a gas. Just after removal from the permeator, a small amount of Hg is injected into the open end of the capillary, sealing the capillary, but leaving the Hg free to move as gas permeates out of the shell. The prepared capillary is then placed inside a sealed glass tube much larger in volume, so that atmospheric pressure variations do not affect the Hg position. By monitoring the position of the Hg, the volume of gas permeating out of the shell is measured as a function of time.

The permeation measurements for one shell are shown in Fig. 34.17. If the pressure inside the shell decreases with time as $\exp(-t/\tau)$, where τ is the time constant to be determined, then the volume of gas diffusing from a shell is

$$V(t) = V_T [1 - \exp(-t/\tau)], \quad (2)$$

where V_T is the total volume of gas from $t = 0$ to time $t \gg \tau$. The



T865

Fig. 34.17

Two permeation tests of a bounce-coated polymer shell with dimensions indicated. The solid lines are fits of the data to Eq. (2). Different permeation pressures were used for the two gases. Values of permeability of plasma-deposited parylene are obtained from the values of τ .

position of the Hg at time t , $x(t)$, can be expressed

$$x(t) = x_0 + V(t)/A, \tag{3}$$

where x_0 is the position at $t = 0$ and A is the cross-sectional area of the capillary. Combining Eqs. (2) and (3), the resulting equation for $x(t)$ is fit by least squares to the measured data. The three fitting parameters are x_0 , V_T , and τ . To plot the data in Fig. 34.17, the $x(t)$ data points were converted to $V(t)$ using Eq. (3) and the value of x_0 obtained from the fit. The data are fit well by Eqs. (2) and (3).

The measured values of τ imply permeabilities of plasma-deposited parylene for He of 7.8×10^{-16} mol/m s Pa and for Ar of 3.3×10^{-17} mol/m s Pa, both at room temperature. (The permeability of polystyrene, an order of magnitude higher for both gases, was taken into account.) The value for He is 7% lower than the value listed for conventional parylene.¹⁵ A value for Ar is not listed. The permeability to Ar is low enough that a shell containing Ar may be removed from the permeator and either used immediately as a target, or else coated with a metal barrier layer while still containing a significant (and predictable) portion of the original pressure. Some targets made by the latter method have been irradiated by the OMEGA laser.

Conclusion

The continuing development of parylene bounce coating has been described, and some of the constraints on process parameters given. The quality and reliability achieved in this process has allowed hundreds of targets to be coated with parylene ablation layers and irradiated by the OMEGA laser. The substantial tensile strength

achieved with bounce-coated parylene layers has useful implications for the design of polymer shell targets. As a permeation barrier, parylene is useful only for gases as large in atomic radius as Ar. When used with another material as a barrier layer, however, such as polyvinyl alcohol or Al, a layer of bounce-coated parylene can provide the necessary strength for holding high internal pressures of D₂ or DT.

ACKNOWLEDGMENT

This work was supported by the U. S. Department of Energy Office of Inertial Fusion under agreement No. DE-FC08-85DP40200 and by the Laser Fusion Feasibility Project at the Laboratory for Laser Energetics, which has the following sponsors: Empire State Electric Energy Research Corporation, New York State Energy Research and Development Authority, Ontario Hydro, and the University of Rochester. Such support does not imply endorsement of the content by any of the above parties.

REFERENCES

1. R. L. McCrory, L. Montierth, R. L. Morse, and C. P. Verdon, in *Laser Interaction and Related Phenomena, Vol. 5*, edited by H. J. Schwartz, H. Hora, M. Lubin, and B. Yaakobi (Plenum, New York, 1981), pp. 713-742.
2. A. K. Burnham, J. Z. Grens, and E. M. Lilley, *J. Vac. Sci. Technol. A* **5**, 3417 (1987).
3. KMS Fusion Inc., Annual Technical Report, 1981.
4. S. M. Gracewski and R. Q. Gram, *J. Vac. Sci. Technol. A* **5**, 2941 (1987).
5. R. Q. Gram, H. Kim, J. F. Mason, and M. Wittman, *J. Vac. Sci. Technol. A* **4**, 1145 (1986).
6. W. L. Johnson *et al.*, *Amer. Chem. Soc. Div. Polym. Chem.* **19**, 544 (1978).
7. S. A. Letts, D. W. Myers, and L. A. Witt, *J. Vac. Sci. Technol.* **19**, 739 (1981).
8. R. Liepins *et al.*, *J. Vac. Sci. Technol.* **18**, 1218 (1981).
9. S. F. Meyer, *J. Vac. Sci. Technol.* **18**, 1198 (1981).
10. W. L. Johnson *et al.*, in *Plasma Polymerization*, edited by M. Shen and A. T. Bell, Vol. 108 of American Chemical Society Symposium Series (American Chemical Society, 1979), p. 315.
11. Union Carbide, parylene technology brochure.
12. H. Kim, T. Powers, and J. Mason, *J. Vac. Sci. Technol.* **21**, 900 (1982).
13. H. Kim and M. D. Wittman, *J. Vac. Sci. Technol. A* **3**, 1262 (1985).
14. E. Lilley, technical memorandum, Lawrence Livermore National Laboratory (unpublished).
15. M. A. Spivack, *Rev. Sci. Instrum.* **41**, 1614 (1970).